Meat and Muscle Biology™

Variations in Intramuscular Fat Content and Profile in Angus × Nellore Steers Under Different Feeding Strategies Contribute to Color and Tenderness Development in *Longissimus thoracis*

Daniel S. Antonelo[1]*, Mariane Beline[2], Saulo L. Silva[2], Juan F. M. Gómez[2], Christina R. Ferreira[3], Xue Zhang[4], Bruna Pavan[2], Larissa A. Koulicoff[2], Alessandra F. Rosa[2], Rodrigo S. Goulart[2], David E. Gerrard[5], Surendranath P. Suman[6], M. Wes Schilling[4], and Julio C. C. Balieiro[1]

[1]College of Veterinary Medicine and Animal Science, University of Sao Paulo, Pirassununga, SP 13635-900, Brazil
[2]College of Animal Science and Food Engineering, University of Sao Paulo, Pirassununga, SP 13635-900, Brazil
[3]Metabolite Profiling Facility, Bindley Bioscience Center, Purdue University, West Lafayette, IN 47907, USA
[4]Department of Food Science, Nutrition and Health Promotion, Mississippi State University, Mississippi State, MS 39762, USA
[5]Department of Animal and Poultry Sciences, Virginia Tech, Blacksburg, VA 24061, USA
[6]Department of Animal and Food Sciences, University of Kentucky, Lexington, KY 40546, USA
*Corresponding author. Email: danielantonelo@usp.br (Daniel S. Antonelo)

Abstract: Muscle from cattle reared under different finishing regimes (grain vs. forage) and with different growth rates may have divergent metabolic signatures that are reflective of their inherent differences in biochemical processes, which may impact their subsequent transformation into high-quality beef. Differences in muscle lipid profiles were characterized in Angus × Nellore crossbred steers, using multiple reaction monitoring profiling, to identify potential metabolic signatures correlated to beef color and tenderness in the *longissimus thoracis* muscle of cattle fed in either a feedlot- or pasture-based system programmed to achieve either a high or low growth rate. A total of 440 lipids were significant, which were related mainly to triglycerides and phosphatidylcholine lipids. Distinct clusters between feeding strategies for the lipid dataset were revealed, which affected glycerolipid metabolism ($P = 0.004$), phospholipid metabolism ($P = 0.009$), sphingolipid metabolism ($P = 0.050$), and mitochondrial beta-oxidation of long-chain saturated fatty acid ($P = 0.073$) pathways. Lipid content and profile differed with feeding strategies, which were related to L^*, a^*, and tenderness. These findings provide a comprehensive and in-depth understanding of lipidomic profiling of beef cattle finished under different feeding strategies and provide a basis for the relationship between lipid content and profiles and beef quality development.

Introduction

Intramuscular fat (IMF), also known as marbling, is one of the most important meat quality traits affecting quality grading, carcass price, and sensory acceptance of meat (Corbin et al., 2015; Silva et al., 2019). Thus, several studies have been conducted to better understand the pathways involved in IMF deposition in order to understand how to manipulate this desirable trait (Campos et al., 2016). Feeding regime impacts animal growth rate and has been related to changes in lipid metabolism, which directly impacts subcutaneous fat and IMF composition (Mwangi et al., 2019; Wicks et al., 2019), and consequently impacts beef color and tenderness (Gagaoua et al., 2018; Hughes et al., 2020; Valenzuela et al., 2020).

Feedlot-fed animals are commonly subjected to a high-energy diet, which provides greater substrate

availability that leads to increased propionate in the rumen and therefore glucose production, which is related to increased muscle and fat deposition (Ladeira et al., 2016; Wicks et al., 2019). In contrast, nutrient intakes are often below animal requirements for maximal growth in a pasture system, which affects animal growth and lean tissue and fat deposition (Mwangi et al., 2019; Wicks et al., 2019). McIntyre et al. (2009) observed that grain-fed animals that experienced a high growth rate (1.34 kg/d) had higher backfat thickness and greater beef marbling scores than grass-fed animals with a low growth rate (0.63 kg/d). Moreover, Koch et al. (2019) reported that lighter (higher $L*$ values) steaks from grain-fed cattle result from higher marbling scores and lipid content of the muscle, which were also associated with more tender beef (Jung et al., 2015). Gómez et al. (2021) indicated that muscle and fat deposition is predominantly due to the finishing regime, and to a lesser extent to growth rate, although the effects of these factors on carcass and beef traits may be cumulative.

Finishing regime (grain vs. forage) and growth rate are often confounded because cattle fed in intensive feeding programs tend to grow at faster rates. Thus, muscle from cattle reared under different finishing systems may have divergent metabolic signatures that are reflective of their inherent differences in biochemical processes, which may impact their subsequent transformation into high-quality beef (Gagaoua et al., 2017). Therefore, in this research, the muscle lipid profiles from cattle differing in growth rate and feeding regime were compared using multiple reaction monitoring (MRM) profiling—a mass spectrometry–based method for small molecule profiling that allows for accelerated discovery of a large number of discriminating molecular features (Xie et al., 2021)—and correlated to beef color and tenderness.

Material and Methods

All experimental procedures involving animal care were conducted in accordance with the Institutional Animal Care and Use Committee Guidelines of the College of Animal Science and Food Engineering at the University of Sao Paulo (protocol approval number 13.1.541.74.0).

Animals, treatments, and handling

Thirty-six contemporary ½ Angus × ½ Nellore crossbred steers (330 ± 30 kg body weight [BW]; aged 12 ± 1 mo) were subjected to a completely randomized experimental design consisting of 4 treatments ($n = 9$ per treatment): (1) feedlot finished, high growth rate (F-H; average daily gain [ADG] projected at 1.5 kg/d); (2) feedlot finished, low growth rate (F-L; ADG projected at 0.9 kg/d); (3) pasture finished, high growth rate (P-H; ADG projected at 0.9 kg/d); and (4) pasture finished, low growth rate (P-L; ADG projected at 0.6 kg/d). Additionally, it was determined that steers would be harvested at a BW of 530 kg prior to the start of the study. Further details about feeding and facilities have been described by Gómez et al. (2021).

Muscle and meat sampling

An average BW of 530 kg was reached within each treatment after 116, 228, 262, and 292 d of feeding with an ADG of 1.51, 0.94, 0.76, and 0.62 kg/d for F-H, F-L, P-H, and P-L animals, respectively, which differed from each other (Gómez et al., 2021). Steers were fasted for 16 h and then transported (1 km and 4 km for feedlot- and pasture-fed animals, respectively) to the abattoir of the College of Animal Science and Food Engineering at the University of Sao Paulo, Pirassununga, Sao Paulo, Brazil. To minimize day-to-day variations, personnel and facility remained constant across the 4 d of harvest. Animals were harvested according to humane procedures as required by Brazilian law.

After carcasses were chilled for 24 h (0°C to 2°C), samples were excised from the *longissimus thoracis* muscle at the 12th and 13th rib level for further pH, total IMF, and lipidomic analysis. All samples were snap frozen in liquid nitrogen and stored at −80°C. One 2.5-cm-thick *longissimus thoracis* sample from each carcass was collected between the 12th and 13th ribs for beef color and shear force instrumental analyses.

Meat quality analysis

Instrumental color. Fresh samples ($n = 9$ per treatment) were exposed to air for 30 min at 4°C to bloom (AMSA, 2012). The meat color was evaluated using the CIELAB system (CIE, 1979) with a portable spectrophotometer model CM2500d (Konica Minolta Brazil, Sao Paulo, Brazil) with standard illuminant D_{65}, a 10° observation angle, and a 30 mm aperture (AMSA, 2012). $L*$ (lightness), $a*$ (redness), and $b*$ (yellowness) values were determined by averaging 3 measurements per sample.

Instrumental shear force. After color measurement, steaks were roasted in an oven equipped with a thermostat adjusted to 170°C (Model F130/L;

Electric Furnaces Golden Arrow Industry and Commerce Ltd., Sao Paulo, Brazil). Internal meat temperatures were monitored using individual thermometers. Once steaks reached an internal temperature of 40°C, steaks were turned and cooked to an internal temperature of 71°C, as recommended by the American Meat Science Association (AMSA, 2015). Steaks were then cooled to 4°C for 12 h, and six 1.27 cm diameter core samples were taken parallel to muscle fiber orientation using a Drill Bench (Model FG-13B, Caracol Trading of Machinery and Tools LTDA, Sao Paulo, Brazil). Shear force was determined on cores using the TMS-PRO texture analyzer (Food Technology Corporation, Sterling, Virginia) coupled with a Warner-Bratzler shear device that was set at a speed of 200 mm/min (AMSA, 2015). Shear force values were determined by averaging the maximum peak force of 6 cores per sample.

Total intramuscular fat analysis. The lipids were extracted by homogenizing (Ultra-Turrax®, T 25 digital; IKA, Campinas, Sao Paulo, Brazil) the muscle samples ($n = 9$ per treatment) with a chloroform:methanol:distilled water (2:1:0.8; v/v/v) solution, and the total IMF was determined by gravimetry, according to a method reported by Bligh and Dyer (1959).

Lipidomic analysis

Lipid extraction. Six samples per treatment were randomly selected, and approximately 50 mg of each was weighed and ground in liquid nitrogen for lipid extraction using a method reported by Bligh and Dyer (1959). Tissue homogenate (300 µL in ultrapure water) was transferred to a new microtube and mixed with 250 µL of chloroform and 450 µL of methanol. This solution was incubated at 4°C for 15 min prior to the addition of 250 µL of chloroform and 250 µL of water, after which centrifugation was performed for 10 min at $16,000 \times g$, forming a 2-phase solution such that the bottom phase contained the lipids (organic phase). The organic phase was transferred to a new tube and dried using a centrifugal vacuum concentrator (Genevac™ miVac; Genevac LTD, Ipswich, UK), and samples were stored at −80°C until further analysis.

Multiple reaction monitoring profiling. Targeted lipid profiling was performed using discovery MRM profiling methods and instrumentation as recently reviewed by Xie et al. (2021). Specifically, dried lipid extracts were diluted in 50 µL of methanol/chloroform 3:1 (v/v) and 250 µL of injection solvent (acetonitrile/methanol/ammonium acetate 300 mM 3:6.65:0.35 [v/v/v]) to obtain a stock solution. Mass

spectrometry data were acquired by flow-injection (no chromatographic separation) from 8 µL of stock solution that was diluted 300x in injection solvent that was spiked with EquiSPLASH™ LIPIDOMIX® Quantitative Mass Spec Internal Standard (0.1 ng/µL of each of the internal standards) prior to being delivered using a micro-autosampler (G1377A) to the ESI source of an Agilent 6410 triple quadrupole mass spectrometer (Agilent Technologies, Santa Clara, California). A capillary pump was connected to the autosampler and operated at a flow rate of 7 µL/min and pressure of 100 bar. Capillary voltage of the instrument was 4 kV, and the gas flow was 5.1 L/min at 300°C.

The MRM-profiling method was used to profile 1,366 MRM related to lipids, from 11 lipid classes. The MRM set included 152 phosphatidylethanolamines (PE), 62 acyl-carnitines (AC), 57 cholesteryl esters (CE), 121 phosphatidylcholines (PC), 27 sphingomyelins (SM), 148 phosphatidylinositols (PI), 152 phosphatidylglycerols (PG), 148 phosphatidylserines (PS), 36 free fatty acids (FFA), 80 ceramides (CER), and 383 triacylglycerols (TG). TG were profiled using parent ions and a product ion related to the presence of specific fatty acyl residues (C16:0, C16:1, C18:0, C18:1, C18:2, and C20:4). The assigned short hand identity, with TG 16:0_36:1 as an example, starts with class (TG) followed by the fatty acyl chain related to the product ion (16:0) and ends with the sum of the carbon:unsaturation number related to the other 2 fatty acyl chains at the TG (e.g., 36:1), as recommended by the Lipid Maps nomenclature group (Liebisch et al., 2020). Phospholipids were identified by their class (PG, PS, PI, PE, or PC), the number of carbon atoms between both esterified fatty acids, and the number of carbon–carbon double bonds present in the molecule, e.g., PE (34:4). Ion intensity data of each MRM per sample were obtained using in-house scripts that were used for subsequent analysis.

Data analysis

Meat quality data were analyzed in a completely randomized design considering treatment (F-H, F-L, P-H, and P-L) as fixed effects and the animal as the experimental unit. Data were analyzed using the PROC MIXED procedure of SAS version 9.4 (SAS Institute Inc., Cary, North Carolina). The least-squares means (LSMEANS) statement was used to calculate the adjusted means for treatment, and the means were compared by Student t test. Differences were considered statistically significant when $P \leq 0.05$ and marginally significant when $0.05 < P \leq 0.10$.

In order to avoid noisy MRM, ion intensities of 1.3-fold or higher than the ion intensity for a blank sample were considered for statistical analysis. Relative ion intensity was calculated for each MRM by dividing its ion intensity by the sum of all ion intensities across the sample. MRM were then assigned to one of 3 lipid classifications: (A) TG; (B) PC, PE, and SM; and (C) AC, CER, DG, FFA, PG, PI, and PS. Using these designations, the following comparisons were made: (1) F-H versus P-L, which simulates differences between traditional beef production systems; (2) F-L versus P-H, which reflects the effect of nutrient type on lipid deposition; and (3) F-H versus F-L and P-H versus P-L, which examine the effect of growth rate on lipid deposition. The effect of treatments on TG distribution in samples was analyzed using 3 distinct groupings for Student t test analysis: (1) total number of carbons (e.g., TG (54)); (2) total number of unsaturation (e.g., (:4)); and (3) total number of unsaturations grouped into 0, up to 2 and more than 3 unsaturations. The relative ion intensities were uploaded to Metaboanalyst 5.0 (https://www.metaboanalyst.ca/) (Chong et al., 2019). Relative ion intensity data were normalized by auto-scaling, and statistical analysis was performed using a Student t test. Moreover, the information of the internal standard was used to obtain the relative quantification of the total TG, total phospholipid, and phospholipid profile according to its class. Differences were considered statistically significant when $P \leq 0.05$ and marginally significant when $0.05 < P \leq 0.10$.

Principal component analysis (PCA) and heatmaps were developed using the differentially abundant lipids for each sample type. Quantitative enrichment analysis were performed using lipid quantification data sets for each treatment. The compound name was standardized according to KEGG, HMDB, or PubChem ID, and the library chosen was the SMPDB (Small Molecule Pathway Database). Correlation analysis was performed between beef quality traits and lipid compounds using the PatternHunter method with the Pearson's correlation applied as a distance measure.

Results

Meat quality analysis

Steaks from F-H animals had higher $L*$ ($P < 0.001$; lighter appearance), $a*$ ($P = 0.002$; increased redness), and $b*$ ($P < 0.001$; increased yellowness) than those from other treatments (Table 1). Steaks from F-H also had higher IMF ($P = 0.001$) deposition than P-H and P-L animals but no differences when compared with F-L animals ($P > 0.05$). F-L animals had higher $L*$ ($P < 0.05$) and similar IMF ($P > 0.05$) than P-H and P-L animals, which did not differ for beef quality traits. In addition, P-H and P-L animals had higher Warner-Bratzler shear force (WBSF; less tender) than F-H and F-L animals ($P < 0.05$).

Lipidomic analysis

Of the 1,366 ion transitions (MRM) scanned, which are tentatively attributed at the lipid species level, 440 were found to have an intensity of at least 1.3-fold higher than the blank sample (injection solvent) (Supporting Information Table S1). These were related mainly to TG (137) and PC (100) lipids.

Relative ion intensity data showed that 107 TG, 39 PC, 8 SM, 6 PE, 5 DG, 3 AC, 2 PG, 1 CER, and 1 CE were differentially abundant ($P < 0.05$) between F-H and P-L animals (Supporting Information Table S2). There were 51 PC, 10 SM, 9 AC, 9 PE, 9 TG, 4 PI, 3 DG, and 2 FFA that were differentially abundant ($P < 0.05$) between F-L and P-H animals (Supporting Information Table S3), whereas there were 80 TG, 15 PE, 14 PC, 7 SM, and 1 DG differentially abundant ($P < 0.05$) lipids between F-H and F-L animals (Supporting Information Table S4). Moreover, 38 PC, 17 PE, 8 AC, 8 SM, 7 TG, 1 CE, 1 DG, 1 FFA, and 1 PS

Table 1. Means ± standard errors of mean and probability (P value) of the effect of finishing regime and growth rate on beef quality

| Trait	F-H	F-L	P-H	P-L	P value
$L*$	$40.3^a \pm 0.72$	$37.0^b \pm 0.72$	$35.0^c \pm 0.67$	$34.7^c \pm 0.62$	<0.001
$a*$	$19.3^a \pm 0.55$	$16.9^b \pm 0.55$	$16.6^b \pm 0.51$	$16.4^b \pm 0.47$	0.002
$b*$	$15.9^a \pm 0.51$	$12.8^b \pm 0.51$	$12.4^b \pm 0.48$	$12.2^b \pm 0.45$	<0.001
Shear force, N	$60.6^b \pm 4.32$	$64.2^b \pm 4.32$	$86.0^a \pm 4.00$	$78.1^a \pm 3.74$	0.004
Intramuscular fat, %	$6.06^a \pm 0.76$	$4.95^{ab} \pm 0.76$	$3.14^b \pm 1.07$	$2.27^b \pm 1.07$	0.001

$^{a–c}$Values within a row with different superscripts differ significantly at $P < 0.05$.

F-H = feedlot finished, high growth rate (GR); F-L = feedlot finished, low GR; P-H = pasture finished, high GR; P-L = pasture finished, low GR.

were differentially abundant ($P < 0.05$) between P-H and P-L animals (Supporting Information Table S5).

Heatmap and PCA analysis revealed distinct clusters in the F-H versus P-L comparison for the lipid subsets A, B, and C (Figure 1A, 1B, and 1C). Distinct clusters based on F-L versus P-H comparison were observed for the lipid subset B (Figure 2B), but an

overlap was observed for the lipid subsets A and C (Figure 2A and 2C). Heatmap and PCA analysis also revealed distinct clusters in the F-H versus F-L comparison for the lipid subset A and B (Figure 3A and 3B), but an overlap was observed for the lipid subset C (Figure 3C). Distinct clusters based on P-H versus P-L comparison were also observed for the lipid subset
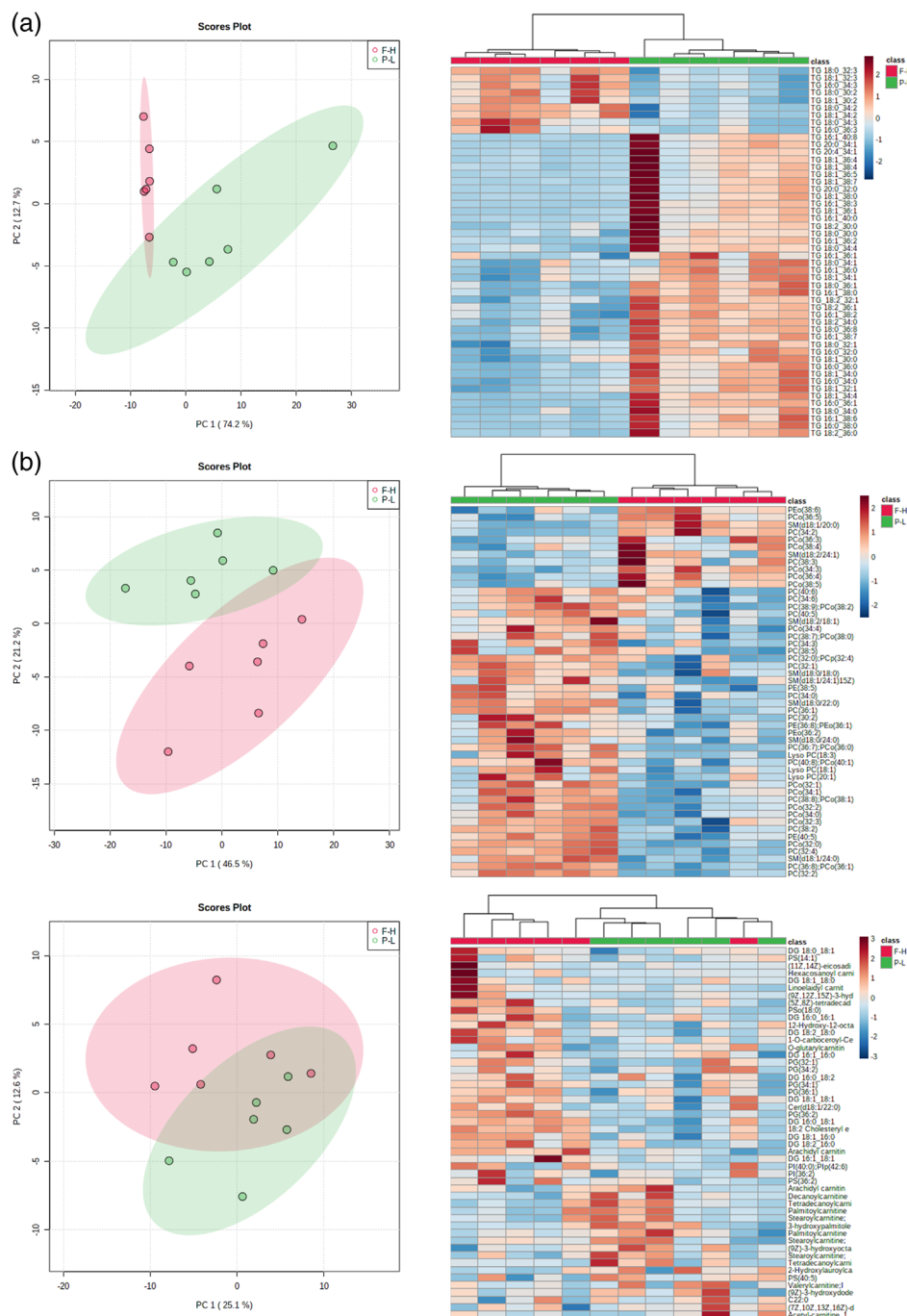
Figure 1. Principal component (PC) analysis scores plot and heatmap analysis (top 25 most informative lipids of each class) of lipidomic distribution based on: (A) triglyceride (TG); (B) phosphatidylcholine (PC), phosphatidylethanolamine (PE), and sphingomyelin (SM); and (C) acyl-carnitine, ceramides (CER), diglyceride (DG), free fatty acids and phosphatidylglycerol (PG), phosphatidylinositol (PI) and phosphatidylserine (PS) between feedlot-finished animals with high growth rate (F-H) and pasture-finished animals with low growth rate (P-L).
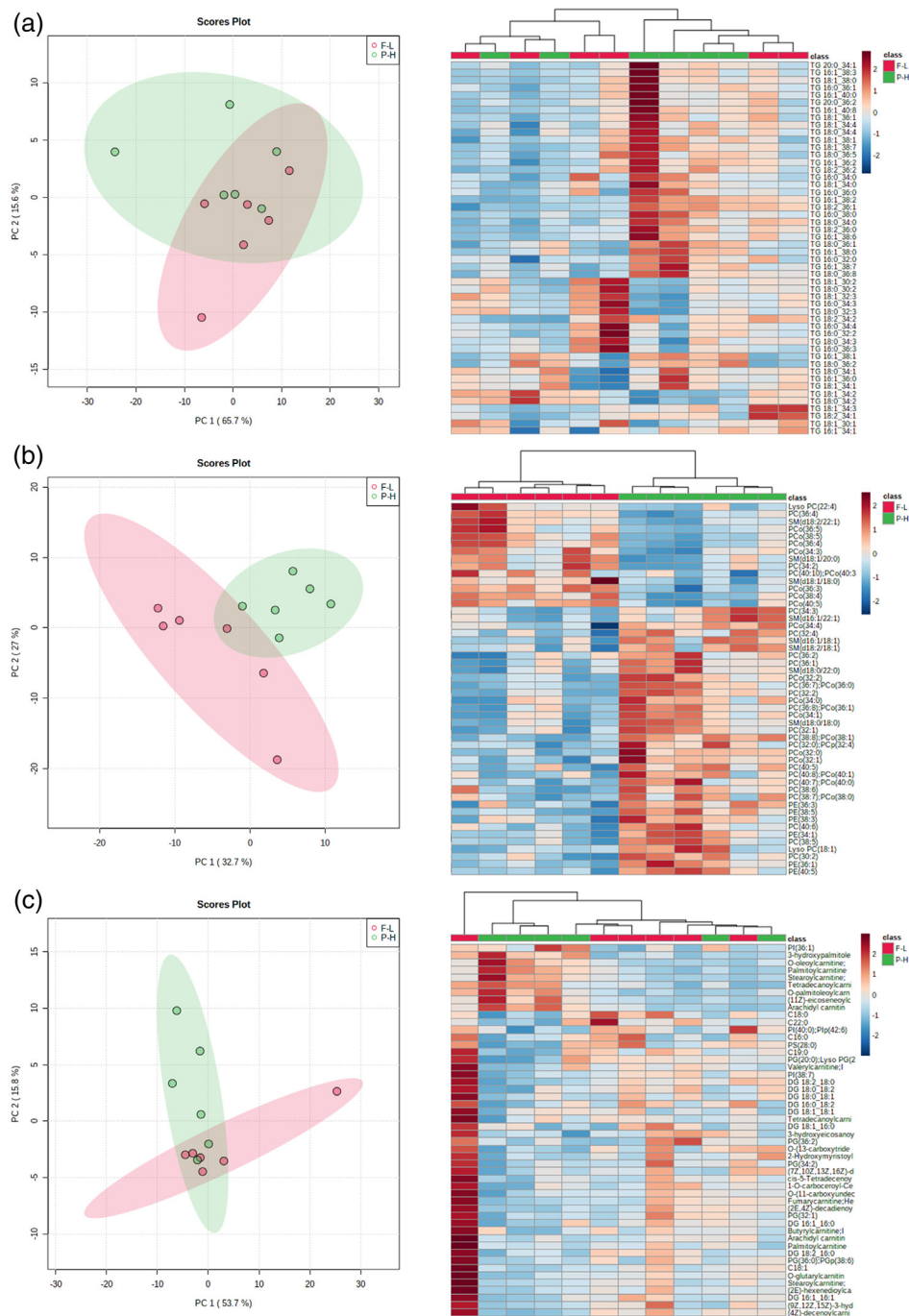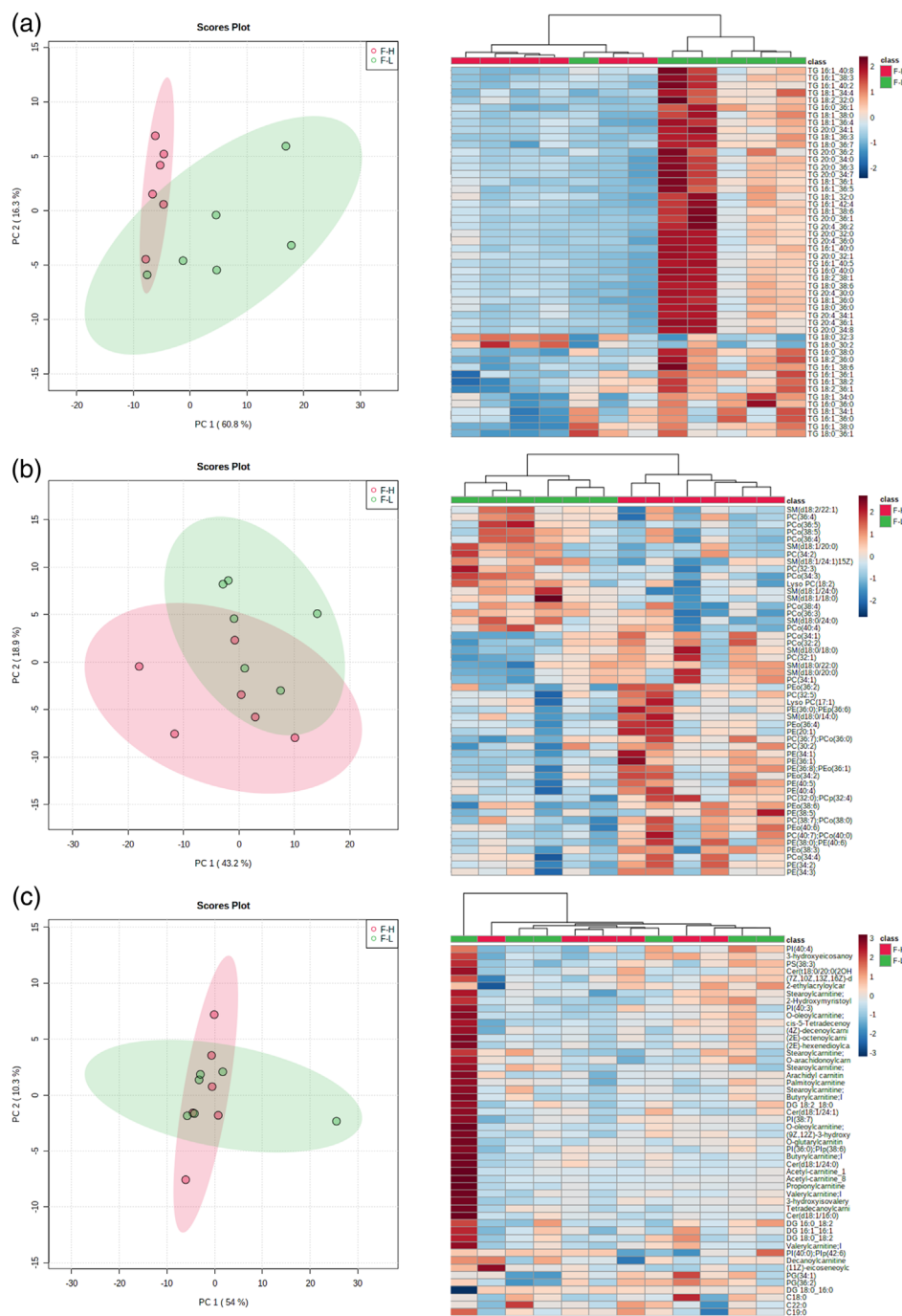
Figure 2. Principal component (PC) analysis scores plot and heatmap analysis (top 25 most informative lipids of each class) of lipidomic distribution based on: (A) triglyceride (TG); (B) phosphatidylcholine (PC), phosphatidylethanolamine (PE), and sphingomyelin (SM); and (C) acyl-carnitine, ceramides (CER), diglyceride (DG), free fatty acids and phosphatidylglycerol (PG), phosphatidylinositol (PI) and phosphatidylserine (PS) between feedlot-finished animals with low growth rate (F-L) and pasture-finished animals with high growth rate (P-H).

B and C (Figure 4B and 4C), but an overlap was observed for the lipid subset A (Figure 4A).

Total TG and TG profile according to the carbon chain length and unsaturation degree is presented in Table 2. F-H steaks had a greater TG concentration than those from other treatments ($P < 0.001$), whereas P-L steaks had less TG than F-L and P-H steaks ($P < 0.05$), which did not differ from each other

($P > 0.05$). F-H steaks also contained a greater concentration of 48-carbon TG than those from other treatments ($P = 0.041$), whereas P-L animals had less 52-carbon ($P = 0.031$) TG and more 56- ($P = 0.027$), 58- ($P = 0.053$), and 64-carbon ($P = 0.043$) TG than other treatments. Moreover, P-L steaks contained a lower concentration of TG with 3 ($P < 0.001$) unsaturations and a higher concentration of TG with 0
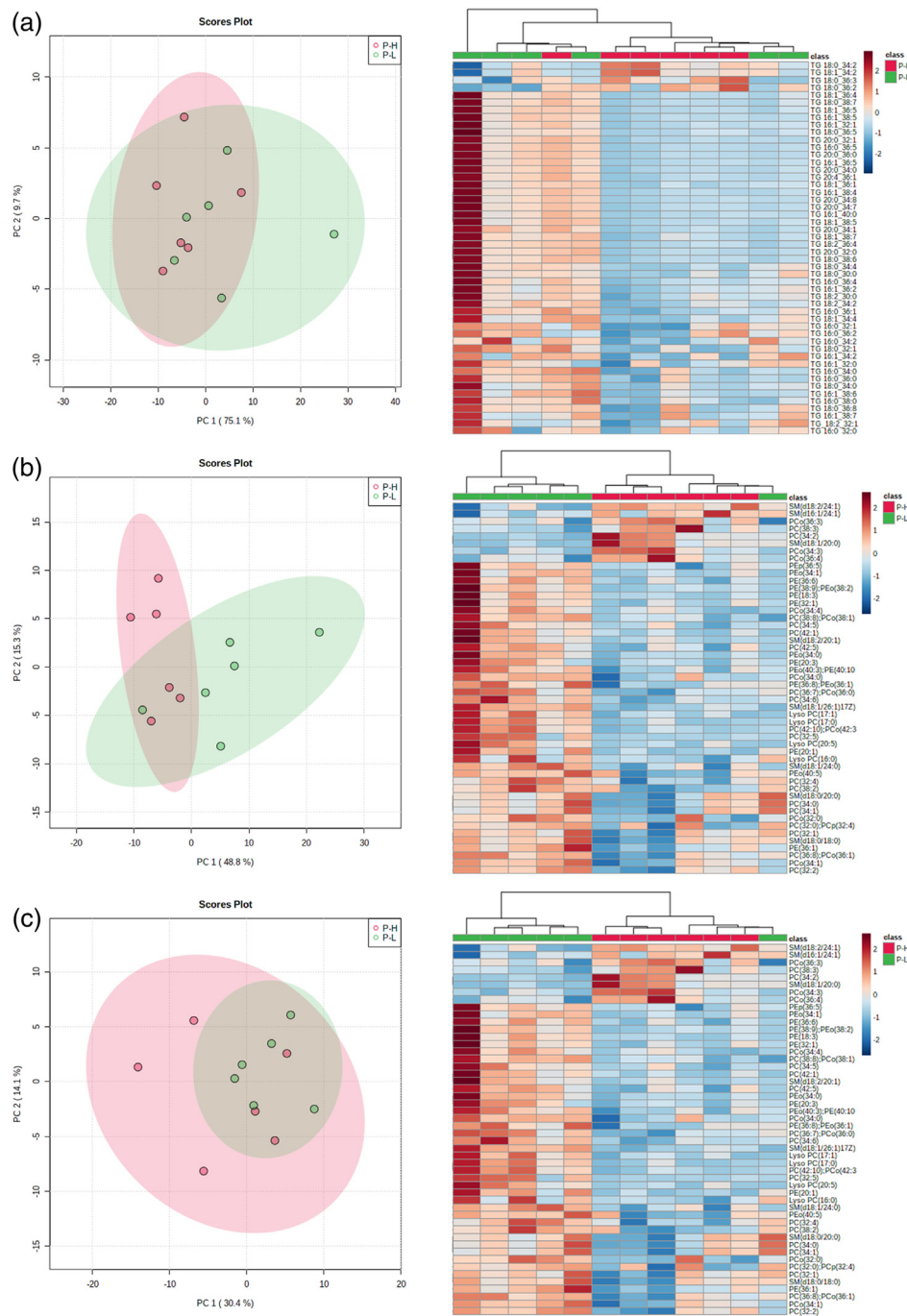
Figure 3. Principal component (PC) analysis scores plot and heatmap analysis (top 25 most informative lipids of each class) of lipidomic distribution based on (A) triglyceride (TG); (B) phosphatidylcholine (PC), phosphatidylethanolamine (PE), and sphingomyelin (SM); and (C) acyl-carnitine, ceramides (CER), diglyceride (DG), free fatty acids and phosphatidylglycerol (PG), phosphatidylinositol (PI) and phosphatidylserine (PS) between feedlot-finished animals with high (F-H) and low (F-L) growth rate.

($P < 0.001$), 1 ($P < 0.001$), 5 ($P = 0.017$), 6 ($P = 0.034$), 7 ($P = 0.010$), 8 ($P < 0.001$), and 9 ($P = 0.022$) unsaturations than F-H and F-L steaks, but they did not differ from P-H steaks in the concentration of TG with 1, 3, and 9 unsaturations ($P > 0.05$). Also, F-H steaks had less TG with up to 2 unsaturations ($P = 0.012$) and more TG with more than 3 unsaturations ($P < 0.001$) when

compared with other treatments. There was no difference in total phospholipids and specific phospholipids among the treatments ($P > 0.05$; Table 3).

Quantitative enrichment analysis revealed that the main metabolic pathways that were affected by feeding regime and growth rate (Figure 5) were glycerolipid metabolism ($P = 0.004$), phospholipid metabolism

Figure 4. Principal component (PC) analysis scores plot and heatmap analysis (top 25 most informative lipids of each class) of lipidomic distribution based on (A) triglyceride (TG); (B) phosphatidylcholine (PC), phosphatidylethanolamine (PE), and sphingomyelin (SM); and (C) acylcarnitine, ceramides (CER), diglyceride (DG), free fatty acids and phosphatidylglycerol (PG), phosphatidylinositol (PI) and phosphatidylserine (PS) between pasture-finished animals with high (P-H) and low (P-L) growth rate.

($P = 0.009$), sphingolipid metabolism ($P = 0.050$), and mitochondrial beta-oxidation of long-chain saturated fatty acids ($P = 0.073$).

Correlation analysis

Seven lipids (3 AC, 2 PC, 1 PE, and 1 SM) had moderate ($-0.4 > r > 0.4$) and significant ($P < 0.05$)

correlation with L^* (Figure 6; Supporting Information Table S6), whereas 43 lipids (featuring 22 TG, 9 AC, and 5 PG) had moderate and significant correlations with a^* (Figure 6; Supporting Information Table S7) and 132 lipids (featuring 85 TG, 27 PC, and 15 PE) were moderately correlated with WBSF (Figure 6; Supporting Information Table S8).

Table 2. Means, standard errors of the mean (SEM), and probability (*P* value) of the effect of finishing regime and growth rate on triglycerides profile evaluated by multiple reaction monitoring profiling

Item	F-H	F-L	P-H	P-L	SEM	*P* value
Total triglycerides, ng/μg muscle tissue	5.15[a]	3.82[b]	3.48[b]	2.23[c]	0.520	<0.001
Carbon number, %						
48	15.44[a]	13.55[b]	12.47[b]	13.29[b]	0.690	0.041
50	13.59	13.60	12.58	13.34	0.565	0.549
52	52.72[a]	53.16[a]	51.71[a]	49.20[b]	0.931	0.031
54	17.32[b]	18.29[b]	21.61[a]	21.49[a]	1.038	0.014
56	0.83[b]	1.22[b]	1.44[b]	2.33[a]	0.328	0.027
58	0.08[b]	0.12[b]	0.14[b]	0.26[a]	0.044	0.053
64	0.03[b]	0.04[b]	0.05[b]	0.09[a]	0.014	0.043
Unsaturation number, %						
0	1.41[c]	1.99[bc]	2.35[b]	3.08[a]	0.219	<0.001
1	11.29[c]	13.63[b]	15.84[a]	16.19[a]	0.515	<0.001
2	41.39	41.66	41.67	39.71	0.650	0.132
3	38.20[a]	34.65[b]	31.94[c]	30.41[c]	0.792	<0.001
4	5.74	5.37	4.85	5.53	0.314	0.255
5	0.44[b]	0.69[b]	0.81[b]	1.33[a]	0.181	0.017
6	0.45[b]	0.63[b]	0.68[b]	1.14[a]	0.158	0.034
7	0.15[b]	0.25[b]	0.29[b]	0.49[a]	0.064	0.010
8	0.84[c]	1.00[c]	1.39[b]	1.83[a]	0.138	<0.001
9	0.09[b]	0.14[b]	0.18[ab]	0.29[a]	0.042	0.022
Grouped unsaturation, %						
Up to 2	52.68[b]	55.28[a]	57.52[a]	55.90[a]	0.930	0.012
More than 3	45.90[a]	42.73[b]	40.13[c]	41.02[bc]	0.892	<0.001

[a–c]Values within a row with different superscripts differ significantly at *P* < 0.05.

F-H = feedlot finished, high growth rate (GR); F-L = feedlot finished, low GR; P-H = pasture finished, high GR; P-L = pasture finished, low GR.

Table 3. Means, standard errors of the mean (SEM), and probability (*P* value) of the effect of finishing regime and growth rate on phospholipids profile evaluated by multiple reaction monitoring profiling

Class, ng/μg muscle tissue	F-H	F-L	P-H	P-L	SEM	*P* value
Phosphatidylcholine	1.267	1.275	1.273	1.267	0.0031	0.146
Phosphatidylethanolamine	0.267	0.273	0.270	0.267	0.0032	0.405
Phosphatidylglycerol	0.030	0.028	0.030	0.027	0.0023	0.690
Phosphatidylinositol	0.065	0.077	0.077	0.062	0.0056	0.149
Phosphatidylserine	0.037	0.042	0.040	0.038	0.0030	0.683
Sphingomyelin	0.288	0.382	0.358	0.278	0.0517	0.423
Total phospholipids	1.953	2.072	2.043	1.937	0.0636	0.377

F-H = feedlot finished, high growth rate (GR); F-L = feedlot finished, low GR; P-H = pasture finished, high GR; P-L = pasture finished, low GR.

Discussion

Intramuscular fat mostly consists of structural lipids, phospholipids, and TG (Listrat et al., 2016), which is the result of the intake of fatty acids through the diet, de novo fatty acid biosynthesis, TG formation, and TG degradation (Nürnberg et al., 1999). IMF content is mainly affected by cattle breed, diet composition, and animal's age (Nürnberg et al., 1999; Mwangi et al., 2019; Wicks et al., 2019) but also depends on the muscle growth rate (Hocquette et al., 2009). In the present study, feeding regime and growth rate impacted IMF deposition, mainly because F-H animals had higher IMF deposition than P-L animals (Table 1). However, under a similar growth rate, F-L and P-H animals had similar IMF deposition, suggesting that diet was the main driver of IMF deposition. Koch et al. (2019) also reported a higher IMF deposition in animals fed high-concentrate diets (higher ADG) when compared with those fed high-quality forages (lower ADG). This is most likely due to increases in propionate from starch-based diets, which is the primary lipid
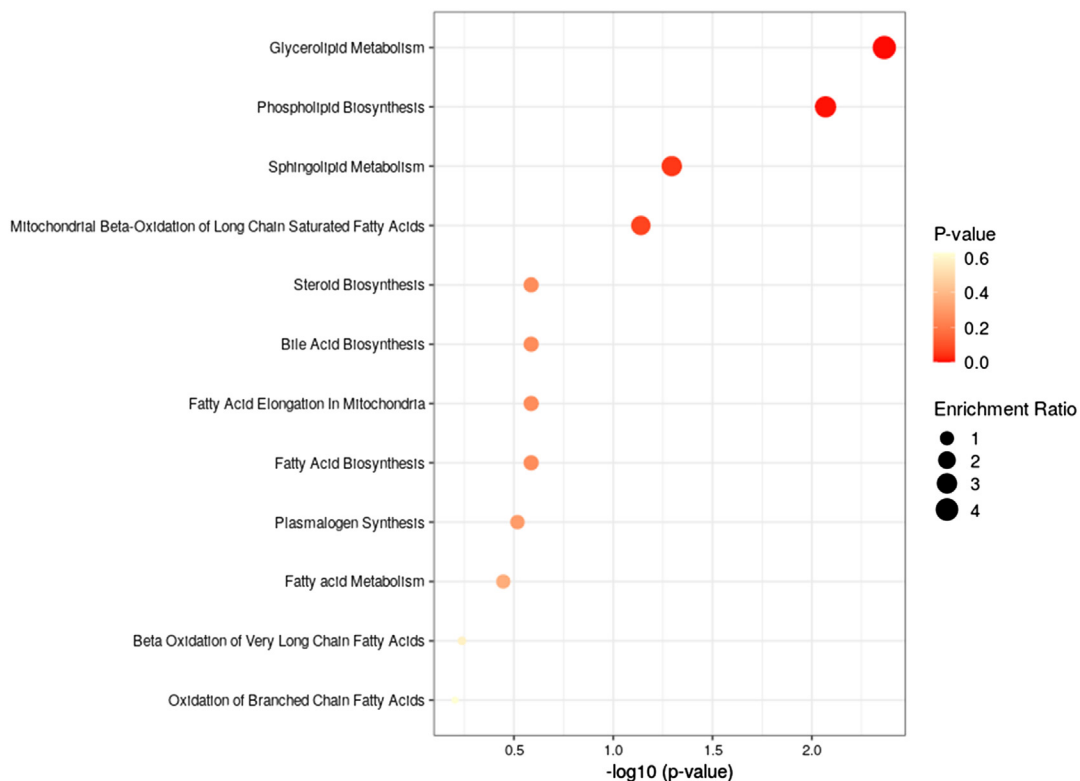
Figure 5. Metabolite sets enrichment according to finishing regime and growth rate.
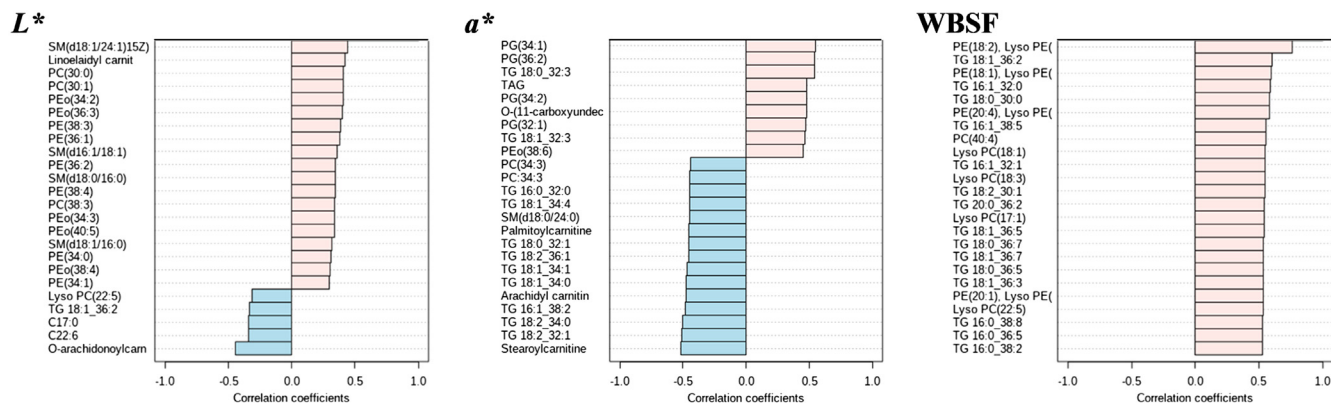

Figure 6. Top 24 lipids that were associated with beef color (*L** and *a**) and Warner-Bratzler shear force (WBSF) using Pearson's correlation as a distance measure.

precursor in intramuscular adipose tissue, compared with acetate from a grass-based diet (Smith and Crouse, 1984). This may also help explain the higher IMF deposition in feedlot animals fed *ad libitum* because there would be even greater amounts of propionate compared with those fed in feedlots to attain slower growth rates comparable to P-L cattle. Therefore, feeding regime or dietary component (grain vs. grass) was the main factor altering IMF deposition.

In this study, F-H steaks had greater total TG deposition than F-L and P-L animals, whereas P-H steaks had greater TG deposition than P-L cattle. In addition, F-H steaks had a higher amount of unsaturated TG, which was mainly due to TG with 3 double bonds compared with other treatments (Table 2). These differences in TG profile may be partially explained by the different requirements of TG mobilization in order to release fatty acids so that they are oxidized in the mitochondrial matrix as a source of energy for animal growth, which may be supported by the impact of treatments on mitochondrial beta-oxidation of the long-chain fatty acids pathway. Ladeira et al. (2016, 2018)

reported that higher levels of glycerol in the muscle, as suggested in F-H animals in the present study, may be indicative of TG hydrolysis, which may support mitochondrial oxidation as lower levels of free carnitine may reflect utilization for long-chain fatty acid transport into the mitochondria. In the present work, F-H animals had higher hexadecanedioic acid mono-L-carnitine ester and stearoylcarnitine concentration than P-L animals (Supporting Information Table S2), which aid in the mechanism whereby long-chain fatty acids are transferred from the cytosol to the mitochondrial matrix to undergo beta-oxidation. Moreover, although F-L animals had greater concentrations of 9 different AC (including elaidic carnitine, O-oleoylcarnitine, palmitoylcarnitine, and cervonyl carnitine) than P-H animals, they had similar TG deposition and profile, except for TG with 1 and 3 unsaturations, which may be attributed to differences in the feeding regime. Therefore, these results may indicate that growth rate had the greatest impact at altering TG deposition and TG profile.

In addition to the neutral lipids primarily consisting of TG, IMF is also composed by polar lipids, containing mostly phospholipids (Legako et al., 2015). Scollan et al. (2014) reported that the overall fat content of the animal and muscle has an important impact on proportionate fatty acid composition because of the different fatty acid composition of TG and phospholipids. Wood et al. (2004) stated that cattle with lower levels of IMF are expected to produce meat with a higher amount of unsaturated fatty acids, which are restricted almost exclusively to the phospholipid fraction. Moreover, Bressan et al. (2016) reported that the IMF profile largely depends on the finishing system, in which grain-fed animals have more saturated fatty acids whereas grass-fed animals have more unsaturated fatty acids. In the present study, despite the higher deposition of IMF and unsaturated TG in F-H steaks compared with other treatments, feeding strategies did not change the concentration of phospholipids or total phospholipid deposited in the lean. However, phospholipid profiles within classification were impacted, in that P-L steaks had greater amounts of most PC, PE, and SM compared with F-H steaks whereas P-H beef had more PC, PE, and SM compared with F-L steaks (Table 3). These data may be explained by changes in the IMF composition caused by the impact of the treatments on the glycerolipid metabolism pathway (Figure 5). Moreover, PC, PE, and SM did not present a clear abundance direction when comparing growth rate within the feeding regime (F-H vs. F-L and P-H vs. P-L). Differences in phospholipid profiles across

treatments may be partially explained by the impact of the treatments on the phospholipid biosynthesis and sphingolipid metabolism pathways (Figure 5). Therefore, these results may indicate that feeding regime (grain vs. pasture) seemed to be the main factor that altered phospholipid profile.

Some MRM from the PC, PE, SM, and AC classes were positively correlated with beef lightness (L^*) (Supporting Information Table S6). Specifically, SM (d18:1/24:1(15Z)) was the most correlated MRM with L^*, in addition to being one of the top 25 MRM clustered to distinguish F-H versus P-L and F-H versus F-L (Figure 1B and 3B, respectively). Interestingly, although SM(d18:1/24:1(15Z)) content was 1.07- and 1.14-fold higher in F-L and P-L when compared with F-H, respectively, lower L^* values were observed in F-L and P-L steaks. The SM(d18:1/24:1(15Z)) is a type of sphingolipid found in animal cell membranes that helps prevent damage to the cell structure (Gault et al., 2010). Hughes et al. (2020) reported that the lipid component of cell membranous structures is believed to be partially responsible for light scattering; thus, microstructural components in muscle cells dictate light scattering and beef lightness. The results of this study suggest that modifications to the cell structure (such as the fluidity of membrane increasing the permeability), mainly in F-H steaks when compared with other treatments, contributes to the light scattering process, in which light is diffused or deflected by collisions with particles of the medium that it transverses. Similarly, Koch et al. (2019) observed lighter steaks from feedlot-fed cattle with higher marbling scores and lipid content within the muscle, because greater IMF deposition alters the muscle structure (Valenzuela et al., 2020). Moreover, Bate-Smith (1948) reported that light scattering is also partially dependent on the texture of the meat surface, which is in agreement with the WBSF data found in this study, where pasture-fed animals produced less tender meat and lower L^* values than feedlot-fed animals.

In the present study, several TG, AC, and PG were correlated with a^* (redness) (Supporting Information Table S7), in addition to being among the top 25 MRM clustered, in their subset lipid, to distinguish between F-H and P-L (Figure 1). The direction of the correlation was observed to be conditional to the MRM concentration in the F-H and P-L groups but not in the F-L and P-H groups, in which the higher concentration in the F-H group compared with the P-L group contributed to a greater correlation. Overall, most of the TG and AC were negatively correlated with a^*, which may suggest that the accumulation of compounds by

oxidation of unsaturated fatty acids and meat phospholipids is correlated with myoglobin oxidation in fresh beef (Faustman et al., 2010). Ramanathan et al. (2020) reported that changes in oxymyoglobin and a^* values appeared to be driven by the oxidation of unsaturated fatty acids in phospholipids and TG. Specifically, in this study, PG(34:1) and PG(36:2) were the most positively correlated MRM with redness, which is in good agreement with their greater abundance in F-H steaks compared with P-L steaks (Supporting Information Table S2). PG(34:1) and PG(36:2) are precursors of cardiolipins, which are plentiful in the intermembrane of mitochondria and suggestive of increased mitochondrial activity (Chen et al., 2018) and presumably critical in achieving and maintaining a bright cherry-red in fresh beef (Ramanathan and Mancini, 2018). Therefore, changes in TG, AC, and PG profiles promoted by increased growth rate may contribute to increased redness in F-H steaks mainly through greater unsaturated fatty acid oxidation and a corresponding increase in mitochondrial activity.

Several TG, PC, and PE were positively correlated with WBSF (Supporting Information Table S8), in addition to being among the top 25 MRM clustered, in their subset lipid, to distinguish between F-H and P-L and between F-L and P-H (Figures 1 and 2, respectively). The WBSF correlation was observed to be conditional to feeding regime, in that the higher the TG, PC, and PE concentration in pasture-fed animals compared with feedlot-fed animals, the higher the correlation observed. Specifically, PE(18:2) was the most positively correlated MRM with WBSF, which belongs to the PE class that is implicated in cellular apoptosis via mitochondrial permeability transition that was initiated by reactive oxygen species (Kaku et al., 2015). Oak et al. (2000) reported that PE degradation generates products that accelerate membrane lipid peroxidation, causing oxidative stress to cells, which positively affects the development of tenderness (Gagaoua et al., 2015). These authors hypothesized that PC hydrolysis at the first stage of postmortem apoptosis may invert membrane polarity (which will induce changes in membrane fluidity, thus increasing the permeability to ions such as Ca^{2+} and increasing the μ-calpain activity) and increase of beef tenderness. The results of the present study may suggest that steaks from feedlot-fed animals underwent higher postmortem degradation of PC and PE than pasture-fed animals. Therefore, although PC and PE concentration were not altered (Table 3), their profiles were modified by feeding regime and contributed to the tenderization of beef.

There are several possible explanations for the positive effect of lipids on tenderness, including the presence of TG within the perimysium in fat cells, which might have a physical effect in the process of tenderization by separating muscle fiber bundles and opening the muscle structure (Wood et al., 2004). Ouali et al. (2013) suggested more active participation of lipids in the tenderizing process through contributing to energy production in the first hours after slaughter, mainly via AMP-activated protein kinase (Scheffler and Gerrard, 2007). Polati et al. (2012) reported an increase of β-hydroxyacyl CoA-dehydrogenase, a member of the beta-oxidation of lipids, which is indicative of TG degradation and may be used as a biomarker of beef tenderness. Therefore, the main reason for the changes in TG and phospholipid profiles (which were caused by the feeding regime) contributing to beef tenderness is not completely clear, but results suggest that TG and phospholipid profiles—and their degradation and signaling—contribute to the development of tender beef.

This study elucidated the effects of feeding regime and growth rate on beef color and tenderness, as well as on the profile of muscle lipids, using a lipidomics approach based on MRM profiling. Lipid content and profile differed from feeding strategies, which were related to L^*, a^*, and tenderness. Overall, results indicate that feeding regime is the main factor that is responsible for altering IMF deposition and phospholipid profiles, which contribute to the development of beef lightness and tenderness. Moreover, growth rate was the main factor that affected TG deposition and profile, which was positively correlated with the redness of the beef. New insights were elucidated on the effects of feeding strategies on lipid profile in beef at class and molecular levels. These findings provide a comprehensive and in-depth understanding of lipidomic profiling of beef cattle finished under different feeding strategies and provide a basis for the relationship between lipid content and profiles and beef quality development.

Acknowledgments

Literature Cited

AMSA. 2012. Meat color measurement guidelines. American Meat Science Association, Champaign, Illinois.

AMSA. 2015. Research guidelines for cookery, sensory evaluation, and instrumental tenderness measurements of meat. 2nd ed. American Meat Science Association, Champaign, Illinois.

Bate-Smith, E. C. 1948. Observations on the phand related properties of meat. J. Soc. Chem. Ind.-L. 67:83–90. https://doi.org/10.1002/jctb.5000670302.

Bligh, E. G., and W. J. Dyer. 1959. A rapid method of total lipid extraction and purification. Can. J. Biochem. Phys. 37:911–917.

Bressan, M. C., E. C. Rodrigues, M. L. Paula, E. M. Ramos, P. V. Portugal, J. S. Silva, R. B. Bessa, and L. T. Gama. 2016. Differences in intramuscular fatty acid profiles among Bos indicus and crossbred Bos taurus × Bos indicus bulls finished on pasture or with concentrate feed in Brazil. Ital. J. Anim. Sci. 15:10–21. https://doi.org/10.1080/1828051X.2016.1139478.

Campos, C. F., M. S. Duarte, S. E. F. Guimarães, L. L. Verardo, S. Wei, M. Du, Z. Jiang, W. G. Bergen, G. J. Hausman, M. Fernyhough-Culver, E. Albrecht, and M. V. Dodson. 2016. Review: Animal model and the current understanding of molecule dynamics of adipogenesis. Animal. 10:927–932. https://doi.org/10.1017/S1751731115002992.

Chen, W. W., Y. J. Chao, W. H. Chang, J. F. Chan, and Y. H. H. Hsu. 2018. Phosphatidylglycerol incorporates into cardiolipin to improve mitochondrial activity and inhibits inflammation. Sci. Rep.-UK. 8:1–14. https://doi.org/10.1038/s41598-018-23190-z.

Chong, J., D. S. Wishart, and J. Xia. 2019. Using MetaboAnalyst 4.0 for comprehensive and integrative metabolomics data analysis. Current Protocols in Bioinformatics. 68:1–128. https://doi.org/10.1002/cpbi.86.

CIE. 1979. Official recommendations on uniform colour space, colour difference equations and metric colour terms. Publication no. 15 (E-1.3.1). Suppl. 2nd ed. Commission Internationale de l'Eclairage, Paris, France.

Corbin, C. H., T. G. O'Quinn, A. J. Garmyn, J. F. Legako, M. R. Hunt, T. T. N. Dinh, R. J. Rathmann, J. C. Brooks, and M. F. Miller. 2015. Sensory evaluation of tender beef strip loin steaks of varying marbling levels and quality treatments. Meat Sci. 100:24–31. https://doi.org/10.1016/j.meatsci.2014.09.009.

Faustman, C., Q. Sun, R. Mancini, and S. P. Suman. 2010. Myoglobin and lipid oxidation interactions: Mechanistic bases and control. Meat Sci. 86:86–94. https://doi.org/10.1016/j.meatsci.2010.04.025.

Gagaoua, M., V. Monteils, S. Couvreur, and B. Picard. 2017. Identification of biomarkers associated with the rearing practices, carcass characteristics, and beef quality: An integrative approach. J. Agr. Food Chem. 65:8264–8278. https://doi.org/10.1021/acs.jafc.7b03239.

Gagaoua, M., B. Picard, J. Soulat, and V. Monteils. 2018. Clustering of sensory eating qualities of beef: Consistencies and differences within carcass, muscle, animal characteristics and rearing factors. Livest. Sci. 214:245–258. https://doi.org/10.1016/j.livsci.2018.06.011.

Gagaoua, M., C. E. M. Terlouw, A. Boudjellal, and B. Picard. 2015. Coherent correlation networks among protein biomarkers of beef tenderness: What they reveal. J. Proteomics. 128:365–374. https://doi.org/10.1016/j.jprot.2015.08.022.

Gault, C. R., L. M. Obeid, and Y. A. Hannun. 2010. An overview of sphingolipid metabolism: from synthesis to breakdown. Adv. Exp. Med. Biol. 688:1–23. https://doi.org/10.1007/978-1-4419-6741-1_1.

Gómez, J. F. M., D. S. Antonelo, M. Beline, B. Pavan, D. B. Bambil, P. Fantinato-Neto, A. Saran-Netto, P. R. Leme, R. S. Goulart, D. E. Gerrard, and S. L. Silva. 2021. Feeding strategies impact animal growth and beef color and tenderness. Meat Sci. 183:108599. https://doi.org/10.1016/j.meatsci.2021.108599.

Hocquette, J. F., I. Cassar-Malek, A. Scalbert, and F. Guillou. 2009. Contribution of genomics to the understanding of physiological functions. J. Physiol. Pharmacol. 60:5–16.

Hughes, J. M., F. M. Clarke, P. P. Purslow, and R. D. Warner. 2020. Meat color is determined not only by chromatic heme pigments but also by the physical structure and achromatic light scattering properties of the muscle. Compr. Rev. Food Sci. F. 19:44–63. https://doi.org/10.1111/1541-4337.12509.

Jung, E. Y., Y. H. Hwang, and S. T. Joo. 2015. Chemical components and meat quality traits related to palatability of ten primal cuts from Hanwoo carcasses. Korean J. Food Sci. An. 35:859–866. https://doi.org/10.5851/kosfa.2015.35.6.859.

Kaku, Y., A. Tsuchiya, T. Kanno, T. Nakano, and T. Nishizaki. 2015. Diarachidonoylphosphoethanolamine induces necrosis/necroptosis of malignant pleural mesothelioma cells. Cell. Signal. 27:1713–1719. https://doi.org/10.1016/j.cellsig.2015.05.007.

Koch, B. M., E. Pavan, N. M. Long, J. G. Andrae, and S. K. Duckett. 2019. Postweaning exposure to high concentrates versus forages alters marbling deposition and lipid metabolism in steers. Meat Muscle Biol. 3:244–253. https://doi.org/10.22175/mmb2018.12.0040.

Ladeira, M. M., J. R. R. Carvalho, M. L. Chizzotti, P. D. Teixeira, J. C. O. Dias, T. R. S. Gionbelli, A. C. Rodrigues, and D. M. Oliveira. 2016. Effect of increasing levels of glycerin on growth rate, carcass traits and liver gluconeogenesis in young bulls. Anim. Feed Sci. Tech. 219:241–248. https://doi.org/10.1016/j.anifeedsci.2016.06.010.

Ladeira, M. M., J. P. Schoonmaker, K. C. Swanson, S. K. Duckett, M. P. Gionbelli, L. M. Rodrigues, and P. D. Teixeira. 2018. Review: Nutrigenomics of marbling and fatty acid profile in ruminant meat. Animal. 12:S282–S294. https://doi.org/10.1017/S1751731118001933.

Legako, J. F., T. T. N. Dinh, M. F. Miller, and J. C. Brooks. 2015. Effects of USDA beef quality grade and cooking on fatty acid composition of neutral and polar lipid fractions. Meat Sci. 100:246–255. https://doi.org/10.1016/j.meatsci.2014.10.013.

Liebisch, G., E. Fahy, J. Aoki, E. A. Dennis, T. Durand, C. S. Ejsing, M. Fedorova, I. Feussner, W. J. Griffiths, H. Köfeler, A. H. Merrill, R. C. Murphy, V. B. O'Donnell, O. Oskolkova, S. Subramaniam, M. J. O. Wakelam, and F. Spener. 2020. Update on LIPID MAPS classification, nomenclature, and shorthand notation for MS-derived lipid structures. J. Lipid Res. 61:1539–1555. https://doi.org/10.1194/jlr.S120001025.

Listrat, A., B. Lebret, I. Louveau, T. Astruc, M. Bonnet, L. Lefaucheur, B. Picard, and J. Bugeon. 2016. How muscle structure and composition influence meat and flesh quality. Sci. World J. 2016:3182746. https://doi.org/10.1155/2016/3182746.

McIntyre, B. L., G. D. Tudor, D. Read, W. Smart, T. J. Della Bosca, E. J. Speijers, and B. Orchard. 2009. Effects of growth path, sire type, calving time and sex on growth and carcass characteristics of beef cattle in the agricultural area of Western Australia. Anim. Prod. Sci. 49:504–514. https://doi.org/10.1071/EA08180.

Mwangi, F. W., E. Charmley, C. P. Gardiner, B. S. Malau-Aduli, R. T. Kinobe, and A. E. O. Malau-Aduli. 2019. Diet and genetics influence beef cattle performance and meat quality characteristics. Foods. 8:1–24. https://doi.org/10.3390/foods8120648.

Nürnberg, K., B. Ender, H. J. Papstein, J. Wegner, K. Ender, and G. Nürnberg. 1999. Effects of growth and breed on the fatty acid composition of the muscle lipids in cattle. Eur. Food Res. Technol. 208:332–335. https://doi.org/10.1007/s002170050425.

Oak, J. H., K. Nakagawa, and T. Miyazawa. 2000. Synthetically prepared Amadori-glycated phosphatidylethanolamine can trigger lipid peroxidation via free radical reactions. FEBS Lett. 481:26–30. https://doi.org/10.1016/S0014-5793(00)01966-9.

Ouali, A., M. Gagaoua, Y. Boudida, S. Becila, A. Boudjellal, C. H. Herrera-Mendez, and M. A. Sentandreu. 2013. Biomarkers of meat tenderness: Present knowledge and perspectives in regards to our current understanding of the mechanisms involved. Meat Sci. 95:854–870. https://doi.org/10.1016/j.meatsci.2013.05.010.

Polati, R., M. Menini, E. Robotti, R. Millioni, E. Marengo, E. Novelli, S. Balzan, and D. Cecconi. 2012. Proteomic changes involved in tenderization of bovine Longissimus dorsi muscle during prolonged ageing. Food Chem. 135:2052–2069. https://doi.org/10.1016/j.foodchem.2012.06.093.

Ramanathan, R., and R. A. Mancini. 2018. Role of mitochondria in beef color: A review. Meat Muscle Biol. 2:309–320. https://doi.org/10.22175/mmb2018.05.0013.

Ramanathan, R., S. P. Suman, and C. Faustman. 2020. Biomolecular interactions governing fresh meat color in post- mortem skeletal muscle: A review. J. Agr. Food Chem. 68:12779–12787. https://doi.org/10.1021/acs.jafc.9b08098.

Scheffler, T. L., and D. E. Gerrard. 2007. Mechanisms controlling pork quality development: The biochemistry controlling post-mortem energy metabolism. Meat Sci. 77:7–16. https://doi.org/10.1016/j.meatsci.2007.04.024.

Scollan, N. D., D. Dannenberger, K. Nuernberg, I. Richardson, S. MacKintosh, J. F. Hocquette, and A. P. Moloney. 2014. Enhancing the nutritional and health value of beef lipids and their relationship with meat quality. Meat Sci. 97:384–394. https://doi.org/10.1016/j.meatsci.2014.02.015.

Silva, L. H. P., R. T. S. Rodrigues, D. E. F. Assis, P. D. B. Benedeti, M. S. Duarte, and M. L. Chizzotti. 2019. Explaining meat quality of bulls and steers by differential proteome and phosphoproteome analysis of skeletal muscle. J. Proteomics. 199:51–66. https://doi.org/10.1016/j.jprot.2019.03.004.

Smith, S. B., and J. D. Crouse. 1984. Relative contributions of acetate, lactate and glucose to lipogenesis in bovine intramuscular and subcutaneous adipose tissue. J. Nutr. 114:792–800. https://doi.org/10.1093/jn/114.4.792.

Valenzuela, J. L., S. S. Lloyd, F. L. Mastaglia, and R. L. Dawkins. 2020. Adipose invasion of muscle in Wagyu cattle: Monitoring by histology and melting temperature. Meat Sci. 163:108063. https://doi.org/10.1016/j.meatsci.2020.108063.

Wicks, J., M. Beline, J. F. M. Gomez, S. Luzardo, S. L. Silva, and D. E. Gerrard. 2019. Muscle energy metabolism, growth, and meat quality in beef cattle. Agriculture. 9:1–10. https://doi.org/10.3390/agriculture9090195.

Wood, J. D., R. I. Richardson, G. R. Nute, A. V. Fisher, M. M. Campo, E. Kasapidou, P. R. Sheard, and M. Enser. 2004. Effects of fatty acids on meat quality: A review. Meat Sci. 66:1–32. https://doi.org/10.1016/S0309-1740(03)00022-6.

Xie, Z., C. R. Ferreira, A. A. Virequ, and R. G. Cooks. 2021. Multiple reaction monitoring profiling (MRM profiling): Small molecule exploratory analysis guided by chemical functionality. Chem. Phys. Lipids. 235:105048. https://doi.org/10.1016/j.chemphyslip.2021.105048.

Supplemental Materials

Supplemental materials for this article are available online at https://doi.org/10.22175/mmb.13043.

Table S1. Lipids profiled by multiple reaction monitoring profiling.

Table S2. Mean, standard error of mean (SEM) and probabilities (P-value) of lipids that differed ($P \leq 0.05$) between feedlot finished animals with high growth rate (F-H) and pasture finished animals with low growth rate (P-L).

Table S3. Mean, standard error of mean (SEM) and probabilities (P-value) of lipids that differed ($P \leq 0.05$) between feedlot finished animals with low growth rate (F-L) and pasture finished animals with high growth rate (P-H).

Table S4. Mean, standard error of mean (SEM) and probabilities (P-value) of lipids that differed ($P \leq 0.05$) between feedlot finished animals with high (F-H) and low growth rate (F-L).

Table S5. Mean, standard error of mean (SEM) and probabilities (P-value) of lipids that differed ($P \leq 0.05$) between pasture finished animals with high (P-H) and low growth rate (P-L).

Table S6. Lipids that were significantly ($P \leq 0.05$) correlated with luminosity ($L*$) using Pearson's correlation as a distance measure.

Table S7. Lipids that were significantly ($P \leq 0.05$) correlated with redness ($a*$) using Pearson's correlation as a distance measure.

Table S8. Lipids that were significantly ($P < 0.05$) correlated with Warner-Bratzler shear force (WBSF) using Pearson's correlation as a distance measure.